

# Propagation Modelling and Propagation Loss Prediction using Wide-Angle Split-Step Fourier Transform Algorithm in Rain Medium

Godwin Effiong<sup>1</sup>, Tebe Larry Ojukonsin<sup>2</sup>, Ayibapreye Kelvin Benjamin<sup>3</sup>

<sup>1</sup>Department of Physics, University of Calabar

<sup>2</sup>Department of Electrical/Electronic Engineering, Niger Delta University

<sup>3</sup>Department of Electrical/Electronic Engineering, Niger Delta University

**Abstract:** *In this paper, wide-angle split step Fourier transform algorithm was used in modelling millimetre wave propagation through rain medium with rain parameters such as rain rate, temperature, drop size distribution, drop radius and effective dielectric constant of rain drops. The split-step Fourier transform method is a range marching technique that is prominent in prediction of electromagnetic wave (EM) propagation in variable terrain and irregular surface. Here, we were able to estimate diffractive and refractive effects due to millimetre wave interaction with rain drops in rain medium using wide-angle parabolic equation (WAPE). MATLAB programming software was used to simulate the numerical WAPE model and plots of field profile versus range and heights shows that attenuation increases with frequency and angle of incidence. We also illustrate that free space pathloss increases due to interaction between EM wave and rain drops. Results obtained were consistent with existing theories.*

**Keywords:** Wide-angle split-step Fourier transform, rain medium, propagation modelling, propagation loss

## 1. Introduction

The split-step Fourier transform is a solution to the parabolic wave equation method which is a range marching technique that is suitable for prediction of electromagnetic (EM) wave propagation in random media and variable terrain. (Benjamin and Bebbington, 2017) modelled a foam-covered sea-surface as slices of sea foam layers using the narrow-angled split-step Fourier transform technique to investigate millimetre wave propagation through these layers.

Attenuation and specific attenuation as functions of incident angles and depth of sea foam layers were reported which evaluates perturbations due to millimetre wave interactions with randomly distributed air-bubbles in different layers of sea foams (Benjamin, 2019). This model was suitable and efficient for long-range, narrow angle propagation with negligible bottom and surface interactions as it assumed a flat sea-surface.

The split-step Fourier algorithm is efficient for solving standard parabolic equation problems since it gained prominence in the early 1970s when it was introduced by Hardin and Tappert (Tappert, 1974). Wide-angled parabolic equations (PEs) are important for solving short-range, deep-water problems and shallow water problems (Benjamin, 2020). EM wave propagation are generally wide-angled for bottom interacting paths in acoustic wave propagation in the ocean.

Collins proposed the split-step Pade's approximation which is the most recent development in terms of efficient PE solution (Collins, 1991). It uses higher order Pade's approximation instead of the square root operators. The essence is to obtain efficiency gain through the use of higher range step. This technique was reported to be more than an

order of magnitude faster than standard finite difference (FD) and finite element (FE) solution technique (Benjamin, 2020).

Wide-angle PEs are evaluated using FD/F where strong speed and density contrast encountered at the water-bottom interface adversely affect the computational efficiency of the split-step Fourier transform method (Levy, 2000). In cases of strong bottom interactions, an excessively fine computational grid is required (Benjamin, 2020). To achieve this, highcomputational efficiency of the split-step Fourier solution is lost. Hence, the wide-angled PEs with FD/FE scheme helps to provide a unified PE solution with better performance prediction as it is more suitable for solving many practical ocean problems (Levy, 2000).

In this study, we adopt the wide-angle split step Fourier transform algorithm to modelling millimetre wave propagation through rain medium with rain parameters such as rain rate, temperature, drop size distribution, drop radius and effective dielectric constant of rain drops.

## 2. Methodology

Li Dexin et. al implemented the forward-backward mixed discrete Fourier transform (DFTM) which uses the first order forward-backward difference formula to substitute for the conventional second order central difference formula to account for the impedance boundary condition (Dexin, Xiuli & Yongshuang, 2011). This idea solves the instability problems associated with it and improves the method in areas such as robustness and efficiency.

To confirm the correctness and applicability of this improved method its germane to verify the simulated results

with conventional methods in different boundary conditions and real terrains.

Here, we consider a cartesian coordinate system  $(x, y, z)$ , with EM incident field propagating in the  $+x$  paraxial direction,  $z$  is the vertical height and  $x$  is the range. From two dimensional (2D) scalar wave equation and using the Feit-Fleck PE approximation, we obtain the Feit-Fleck PE equation in the 2D range height as follow;

The Feit and Fleck approximation yields

$$Q \sim \sqrt{1+A} + \sqrt{1+B} - 1 \quad (1)$$

Equation (1) is exact in vacuum. For a case of homogeneous medium where  $n = 1 + \delta n$ . The pseudo-differential operator  $Q$  can be expressed as

$$Q \sim \sqrt{1+A+B} = \sqrt{1+A} + \sqrt{1+B} - 1 \quad (2)$$

and

$$Q = 1 + \delta n + \sqrt{1 + \frac{1}{k^2} \frac{\partial^2}{\partial z^2}} - 1 \quad (3)$$

Substituting the expression of  $Q$  in (3) into the expression below for forward travelling wave

$$\frac{\partial u}{\partial x} = -ik(1 - Q)u \quad (4)$$

gives

$$\frac{\partial u}{\partial x} = -ik \left( 1 - (1 + \delta n + \sqrt{1 + \frac{1}{k^2} \frac{\partial^2}{\partial z^2}} - 1) \right) u \quad (5)$$

Substitute  $\delta n = n - 1$  into equation (5) gives

$$\frac{\partial u}{\partial x} = -ik \left( 1 - (1 + (n - 1) + \sqrt{1 + \frac{1}{k^2} \frac{\partial^2}{\partial z^2}} - 1) \right) u \quad (6)$$

This is further expanded to yield

$$\frac{\partial u}{\partial x} = ik \left( (n - 1) + \sqrt{1 + \frac{1}{k^2} \frac{\partial^2}{\partial z^2}} - 1 \right) u \quad (7)$$

The split-step Fourier solution is obtained by solving successively for the refractive and diffractive terms. Using the simplest split, the formal solution is given by

$$\frac{\partial u(x, z)}{\partial x} = ik \left( \sqrt{1 + \frac{1}{k^2} \frac{\partial^2}{\partial z^2}} - 1 \right) u(x, z) + ik(m - 1)u(x, z) \quad (8)$$

The scalar  $u(x, z)$  is the electromagnetic field at random locations,  $k = \frac{2\pi}{\lambda}$  is the wavenumber in vacuum and  $\lambda$  is the free space wavelength,  $m = n + \frac{z}{a_e}$  is the modified

atmospheric refractive index and  $a_e$  is the equivalent earth radius. The formal solution by the SSFT method becomes

$$u(x, z) = e^{ik(n-2+\frac{z}{a_e})\Delta x} F^{-1} \left( e^{i\Delta x \sqrt{k^2 - p^2}} F(u(x_0, z)) \right) \quad (9)$$

In this equation,  $M = e^{i\Delta x \sqrt{k^2 - p^2}}$  denotes the diffraction effects of obstacles in the path,  $N = e^{ik(n-2+\frac{z}{a_e})\Delta x}$  reflects the refraction effects of the media.  $F$  and  $F^{-1}$  indicate the Fourier transformation and inverse transformation respectively.

## 2.1. PE Initial Fields

The split-step PE method must be initialized with a starting field distribution  $(x_0, z)$  at some distance  $x_0$  from the source, since the parabolic wave equation is not valid in the source region. To compute the initial fields there are two options available. First, the initial  $z$  - space field is obtained by analytical method taking free space conditions into consideration and treating the source as a point source radiator. This approach has its drawbacks for highly directional antennas.

Secondly, we can use duality of the antenna field distribution and radiation pattern functions. In vacuum, the antenna radiation pattern function  $f(p)$  and the antenna field distribution  $A(z)$  are Fourier transform pair given as

$$f(p - p_0) = \int_{-\infty}^{\infty} A(z) e^{-i(p-p_0)z} dz \quad (10)$$

where  $p = k_0 \sin \theta$  and  $p_0 = k_0 \sin \theta_0$ ,  $\theta$  denotes the elevation angle along the horizontal and  $\theta_0$  is the antenna main lobe vertical pointing direction (antenna tilt).

For a Gaussian antenna radiation pattern with functional form

$$f(t) = e^{-a^2 t^2} \quad (11)$$

where  $a^2 = \ln 2 / 2$ , and  $t = \frac{\sin \theta - \sin \theta_0}{\sin \frac{\theta_{bw}}{2}} = \frac{p - p_0}{p_1 / 2}$

we can write  $f(p)$  as

$$f(p) = e^{-\ln 2 / 2 \left( \frac{p - p_0}{p_1 / 2} \right)^2} \quad (12)$$

We formulate the even and odd  $p$ -phase fields from the antenna pattern function. The fields are expressed as

$$\psi_e = f(p)e^{-ipz_0} + f(-p)e^{+pz_0} \quad (13)$$

which obeys Dirichlet's boundary condition and

$$\psi_o = f(p)e^{-ipz_0} - f(-p)e^{+pz_0} \quad (14)$$

which obeys Neumann's boundary conditions.

The Fourier shift theorem  $f(p) \rightarrow f(p - p_0)$  is used to properly account for a non-zero source altitude.

Taken the even and odd symmetry  $p$ -space fields, the corresponding  $z$ -space PE field is obtained by taking the inverse cosine or sine cosine of (13) and (14) respectively.

$$\psi_e(0, z) = IFFT[\psi_e(0, p)] \quad (15)$$

$$\psi_o(0, z) = IFFT[\psi_o(0, p)] \quad (16)$$

## 2.2. Wide-angle SSFT Algorithm Steps

- 1) Compute the initial field profile using the inverse Fourier transform (IFFT) of the Gaussian antenna radiation pattern with specific height  $z_0$ , beamwidth  $\theta_{bw}$ , and tilt or elevation angle  $\theta_{tilt}$ .
- 2) Include boundary conditions in the initial field expression. Here, we use Dirichlet or Neumann boundary conditions.
- 3) Compute the refractive index of rain medium with refractivity profile.
- 4) Apply forward Fourier transform (FFT) on initial field profile.
- 5) Multiply the FFT on field profile by  $p$ -space propagator ( $e^{i\Delta x \sqrt{k^2 - p^2}}$ ).
- 6) Apply inverse Fourier transform (IFFT) on the product of  $p$ -space propagator and (FFT) on initial field profile.
- 7) Multiply (IFFT) on the product of  $p$ -space propagator and (FFT) on initial field profile by  $z$ -space propagator ( $e^{ik(n - 2 + \frac{z}{a_e})\Delta x}$ ).
- 8) Check if final range  $x$  is reached else set new old field profile and new initial field profile and repeat steps 1 to 7 until final range is obtained.

## 3. Results and Discussions

A 1-D wide-angled PE algorithm was developed, simulated and tested for evaluation of diffraction effects due to millimetre wave interaction with rain drops above the earth surface. Tests and comparisons of propagated field as a function of range and height were performed.

A Gaussian source field that is horizontally and vertically polarized at  $z_s = 100$  m, with a beamwidth of  $1^\circ$ , elevation or tilt angle  $1^\circ$ , and frequency 300 GHz.

Figures 1 and 2, illustrate field profile of propagated field as a function of range and height for both horizontal and vertical polarization. The figures show that excellent

agreement was obtained and both cases can be used to model a complex propagation environment above the earth's surface in a variable terrain.

The figures below show diffraction and reflection effects through the range 0 – 1.5 km above the earth's surface with maximum height 100 m for horizontal and vertical polarization. We can see that diffuse reflections increases with increase in height of the earth surface.

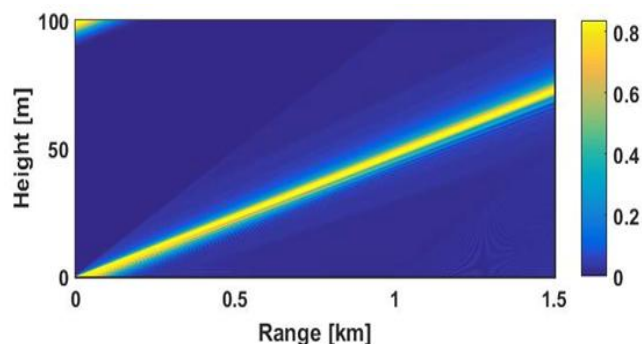


**Figure 1:** Field profile above the earth's surface at maximum height 100 m for horizontal polarization

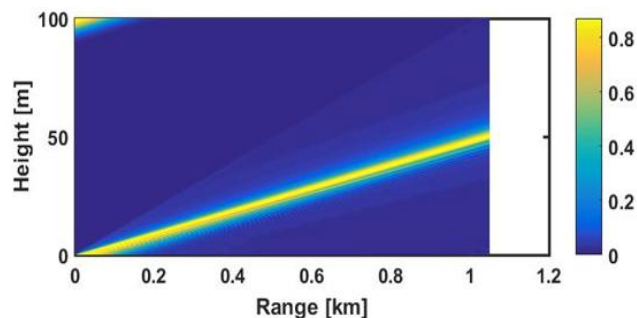


**Figure 2:** Field profile above the earth's surface at maximum height 100 m for vertical polarization

Figure 3 and 4 illustrate the propagation loss (PL) as a function of range in rain medium with maximum height  $z = 100$  m for both horizontal and vertical polarization. The field profiles vary similarly in both cases for maximum range  $x = 1$  km and  $x = 5$  km. The flat earth surfaces show less diffuse reflections than irregular terrains assumed to be wet as shown in both cases of horizontal and vertical polarizations.

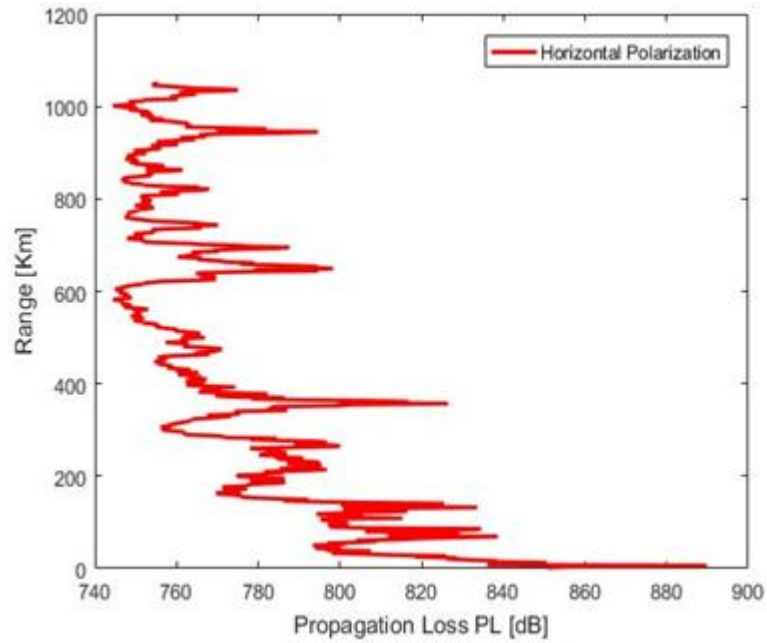


**Figure 3:** Propagation loss (PF) versus range (km) above the earth's surface with rain rate 0.2369 mm/hr

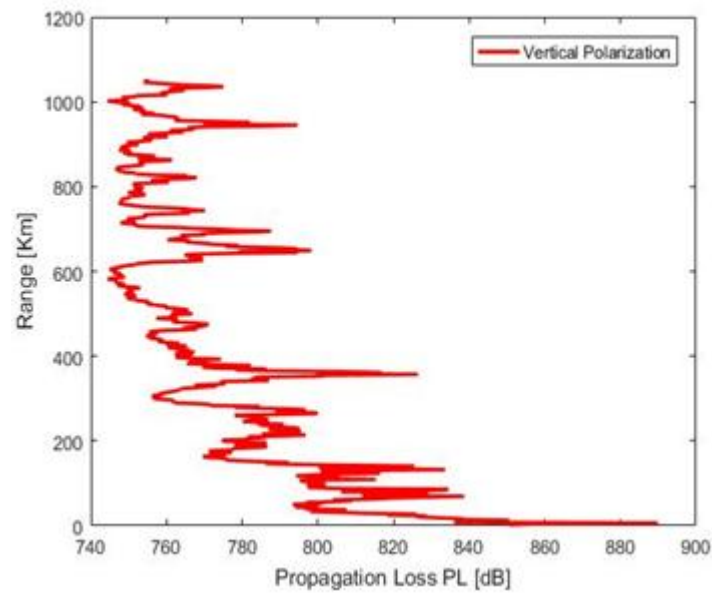


**Figure 4:** Propagation loss (PF) versus range (km) above the earth's surface with rain rate 0.2369 mm/hr

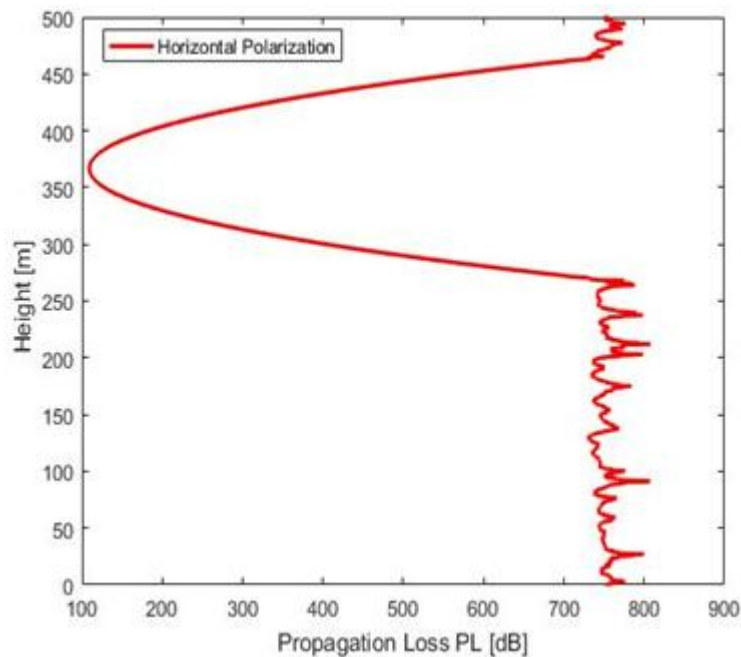


**Figure 5:** Propagation loss (PF) versus height (m) above the earth's surface with rain rate  $0.2369 \text{ mm/hr}$

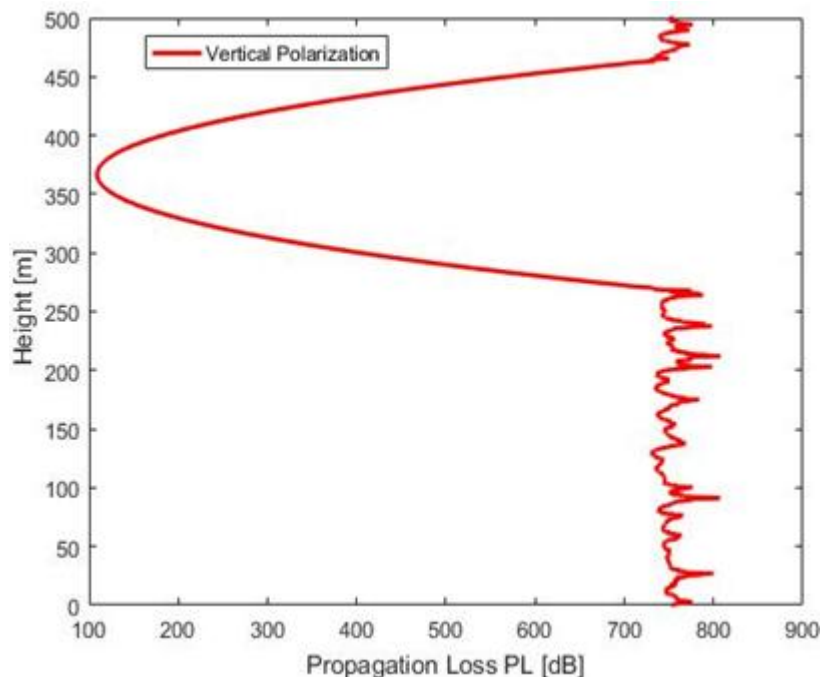


**Figure 6:** Propagation loss (PF) versus height (m) above the earth's surface with rain rate  $0.2369 \text{ mm/hr}$

Figure 5 and 6 illustrate the propagation loss (PL) as a function of range in rain medium with maximum height  $z = 500 \text{ m}$  for both horizontal and vertical polarizations. The field profiles vary similarly in both cases for maximum height  $z = 500 \text{ m}$ . The flat earth surfaces show less diffuse reflections than irregular terrains assumed to be wet as shown in both cases of horizontal and vertical polarizations. The propagation loss is highest at range  $x = 800 \text{ km}$  and lowest at  $= 0 \text{ km}$ . This explains that low altitudes, multipath propagation effects are not significant.

#### 4. Conclusions

The wide-angled PE model requires smaller range steps than the narrow-angled PE and thus takes long computation times when long range propagation is needed. The computation time for wide-angled PE can be at least 12 times longer than that of narrow-angled PE. Hence, the number of nodes used in the transverse and range coordinates should be optimized in respect to the following parameters: frequency of propagation, variable terrain structure, inhomogeneous atmosphere, and choice of the initial antenna pattern specified by its height, beamwidth, elevation or tilt angle. Wide-angled PEs can handle most boundary conditions at the surface more easily than the narrow-angled PEs.

## References

- [1] Benjamin, A. K., & Bebbington, D. O. (2017, November). Millimeter-wave propagation and attenuation in closed packed sea-foam layer and complex dielectric constant of sea-foam using split-step Fourier transform. In *2017 Progress in Electromagnetics Research Symposium-Fall (PIERS-FALL)* (pp. 2556-2563). IEEE.
- [2] Benjamin, A. K. (2019). *Evaluation of millimetre-wave coherent scattering from a sea surface covered by foam modelled as sequences of thin phase-scattering screens using split-step Fourier method* (Doctoral dissertation, University of Essex).
- [3] Benjamin, A. K., & OUSERIGHA, C. E. (2020). Extinction of Millimeter wave on Two Dimensional Slices of Foam-Covered Sea-surface. *International Journal of Scientific Research and Development*, 3(4).
- [4] Collins, M. D. (1991). Higher-order Padé approximations for accurate and stable elastic parabolic equations with application to interface wave propagation. *The Journal of the Acoustical Society of America*, 89(3), 1050-1057.
- [5] Dexin, L., Xiuli, Z., & Yongshuang, S. (2011, July). Prediction of radio wave propagation over irregular terrain by the improved DMFT algorithm. In *Proceedings of 2011 Cross Strait Quad-Regional Radio Science and Wireless Technology Conference* (Vol. 1, pp. 75-78). IEEE.
- [6] Levy, M. (2000). *Parabolic equation methods for electromagnetic wave propagation* (No. 45). IET.
- [7] Tappert, F. D. (1974). Parabolic equation method in underwater acoustics. *The Journal of the Acoustical Society of America*, 55(S1), S34-S34.